Redox rhythm reinforces the circadian clock to gate immune response

Mian Zhou[1,2,*,†], **Wei Wang**[1,2,*,†], **Sargis Karapetyan**[3], **Musoki Mwimba**[1,2], **Jorge Marqués**[1,2], **Dr. Nicolas E. Buchler**[2,3,††], and **Dr. Xinnian Dong**[1,2,††]

[1]Howard Hughes Medical Institute-Gordon and Betty Moore Foundation

[2]Department of Biology, PO Box 90338, Duke University, Durham, North Carolina 27708, USA

[3]Department of Physics, Duke University, Durham, North Carolina 27708, USA

Abstract

Recent studies have shown that in addition to the transcriptional circadian clock, many organisms, including *Arabidopsis,* have a circadian redox rhythm driven by the organism's metabolic activities[1–3]. It has been hypothesized that the redox rhythm is linked to the circadian clock, but the mechanism and the biological significance of this link have only begun to be investigated[4–7]. Here we report that the master immune regulator NPR1 (non-expressor of pathogenesis-related gene 1) of *Arabidopsis* is a sensor of the plant's redox state and regulates transcription of core circadian clock genes even in the absence of pathogen challenge. Surprisingly, acute perturbation in the redox status triggered by the immune signal salicylic acid (SA) does not compromise the circadian clock but rather leads to its reinforcement. Mathematical modelling and subsequent experiments show that NPR1 reinforces the circadian clock without changing the period by regulating both the morning and the evening clock genes. This balanced network architecture helps plants gate their immune responses towards the morning and minimize costs on growth at night. Our study demonstrates how a sensitive redox rhythm interacts with a robust circadian clock to ensure proper responsiveness to environmental stimuli without compromising fitness of the organism.

Life on Earth has evolved the circadian clock to anticipate diurnal and seasonal changes[8]. This "scheduling" mechanism coordinates biological processes to reduce random energy expenditures and increase fitness. In *Arabidopsis*, the daily time-keeping is driven by three interlocked transcription-translation feedback loops (TTFLs): the core loop, the morning loop, and the evening loop. The core loop consists of three transcription factors (TFs): two partially redundant morning-phased CIRCADIAN CLOCK ASSOCIATED 1 (CCA1) and LATE ELONGATED HYPOCOTYL (LHY), and the evening-phased TIMING OF CAB2 EXPRESSION 1 (TOC1). CCA1/LHY and TOC1 are repressors of each other's expression[9,10]. Besides the TTFL circadian clock, non-transcriptional redox oscillations exist in all domains of life, including *Arabidopsis*[3]. Even though redox rhythm was shown to influence the TTFL clock[3], how these two oscillatory systems are linked molecularly and what the biological significance of having two oscillatory systems is remain largely unknown.

To begin addressing these questions, we examined the daily changes in the reduction-oxidation coenzymes NADPH and NADP$^+$ in *Arabidopsis* under constant light and found them to display circadian rhythms ($P < 10^{-4}$), with NADPH peaking before subjective dawn and NADP$^+$ peaking before subjective dusk (Fig. 1a, b). Moreover, their ratio also oscillated in a circadian manner (Extended Data Fig. 1). These data support the existence of widespread metabolic and redox rhythms in plants beyond the previously reported oscillations of oxidized peroxiredoxin, H_2O_2 and catalases[3,7,11]. It is known that the plant immune-inducing signal salicylic acid (SA) can alter the cellular redox to trigger defence gene expression[12]. We found that under constant light, treating plants with SA could significantly perturb NADPH and NADP$^+$ rhythms as well as their ratio (Fig. 1a, b and Extended Data Fig. 1), indicating that the redox rhythm is sensitive to external perturbations.

We next examined whether this SA-triggered redox rhythm perturbation could be transduced to the circadian clock by first focusing on the evening-phased *TOC1*, which is responsive to many environmental factors[13]. Using quantitative PCR (qPCR), we observed significant increases in amplitude and average expression of *TOC1* upon SA treatment (Fig. 1c). Similar results were observed using a transgenic line carrying a reporter of the *TOC1* promoter fused to luciferase (*TOC1p:LUC*)[14] (Fig. 1d, e and Extended Data Fig. 2a). Strikingly, the period of the *TOC1p:LUC* expression rhythm did not change regardless of whether SA was applied at subjective dawn (Fig. 1d) or dusk (Fig. 1e).

To study the effect of endogenous SA, which oscillates in a circadian manner[15], on the clock, we crossed the *TOC1p:LUC* reporter into the SA biosynthesis mutant, *sid2* (*SA induction–deficient 2*)[16]. We found that the amplitude and the average expression of *TOC1* were significantly reduced in *sid2* and this phenotype was rescued upon exogenous SA treatment (Extended Data Fig. 2b). Our results indicate that endogenous SA plays a part in the redox rhythm that modulates the amplitude and average expression of the circadian clock.

SA-induced redox changes can lead to reduction of the master immune regulator, NPR1, the release of NPR1 monomer for nuclear translocation, defence gene induction[12] and subsequent degradation mediated by the nuclear SA receptors NPR3 and NPR4[17]. To test

whether the SA-mediated regulation of *TOC1* is through NPR1, we crossed *TOC1p:LUC* into the *npr1* mutant[18]. We found that the mutation not only dampened the basal expression of *TOC1* but also abolished the SA-triggered increases in expression regardless of the time of treatment (Fig. 2a and Extended Data Fig. 3a–c).

We hypothesized that NPR1 is an intrinsic regulator of *TOC1* in response to the rhythmic accumulation of the endogenous SA[15]. Through western blotting, we indeed found a circadian oscillatory pattern for the NPR1 monomer ($P < 0.01$) with a peak at night (Fig. 2b and Extended Data Fig. 4a). Therefore, oscillation in the endogenous SA level may drive the rhythmic nuclear translocation of NPR1 to regulate the circadian clock genes. To test this hypothesis, we used mutants of cytoplasmic-localized thioredoxins (TRX), *trx-h3* and *trx-h5*, in which NPR1 nuclear translocation is largely impaired[19]. We found that both the basal rhythm of *TOC1p:LUC* and its responsiveness to SA were diminished in *trx-h3 trx-h5* (Fig. 2c and Extended Data Fig. 5a), suggesting the requirement of NPR1 nuclear translocation in regulating *TOC1* expression. Besides SA, glutathione reduced ethyl ester (GSHmee), a redox-altering reagent[20], could also enhance *TOC1* expression in an NPR1-dependent manner (Extended Data Fig. 5b), suggesting that NPR1 is a general redox sensor in modulating this clock gene.

NPR1 is a transcription cofactor of the TGA class of TFs in SA-induced defence gene expression[21]. Using yeast one-hybrid assay, six *Arabidopsis* TGAs were found to have strong binding affinities to the *TOC1* promoter at the two TGA-binding sites (TBS) (Fig. 2d). To confirm this *in planta*, we mutated TBS in the *TOC1p:LUC* reporter (*TOC1p (TBSm):LUC*) and transformed it into *Arabidopsis*. We found that these mutations significantly inhibited transcription of the reporter ($P < 0.001$), indicating that TGAs are transcription activators of *TOC1* (Fig. 2e). A direct role that NPR1/TGA plays in regulating *TOC1* expression was further confirmed through chromatin immunoprecipitation (ChIP) in which association of NPR1 to TBS in the *TOC1* promoter was significantly enhanced upon SA induction (Fig. 2f).

TOC1 is unlikely the only clock gene regulated by NPR1, because lowering the *TOC1* level shortens the clock period while elevating the level lengthens the period[22,23]. However, no such perturbation was observed in *npr1* (Extended Data Fig. 3d) or after SA treatment (Fig. 1d, e). Moreover, SA treatment at dawn should have caused an immediate induction in *TOC1* expression instead of a 12-hour delay (Fig. 1d). To systematically search for other NPR1-targeted clock genes, we performed mathematical modelling using the P2012 circadian model[13] under the assumption that NPR1 is also a transcriptional activator of other clock genes (X and Y in Fig. 3a) (see Methods and Extended Data Figs. 6 and 9 for details).

We first optimized the P2012 model to fit the *TOC1* expression in *npr1* (Fig. 2a), which was a single parameter fit (i.e., basal expression in the absence of functional NPR1). The heat map of the best least-squares fit showed a characteristic "crosshair" pattern centred on *PSEUDO-RESPONSE REGULATOR 7* (*PRR7*) (Fig. 3b), indicating that the basal regulation of *PRR7* by NPR1 best explains the unchanged *TOC1* period in *npr1* (Extended Data Fig. 6a, b). This prediction was verified using qPCR in which *PRR7* transcript levels in *npr1* were found to be significantly lower compared to wild type (Fig. 3c). The second fitting for

SA-induction data involved multiple parameters. We used our fixed basal expression parameter and NPR1 western data (Fig. 2b and Extended Data Fig. 4) to fit the *TOC1* expression from Fig. 2a. The resulting heat map showed a "crosshair" pattern for *LHY/CCA1* (Fig. 3d), suggesting that either one or both of these genes is responsive to SA through the function of NPR1. Using qPCR, we found that while *CCA1* and *EARLY FLOWERING 3* (a negative control) did not respond to SA, the amplitude of *LHY* expression was significantly elevated by SA ($P < 0.05$) (Extended Data Fig. 6c–e) as predicted by our model. This result was further confirmed using the *LHYp:LUC* reporter (Fig. 3e). Consistently, the amplitude of basal *LHY* expression was reduced in *npr1* ($P < 0.05$) while that of *CCA1* remained unchanged (Extended Data Fig. 6f, g). Because LHY is an antagonist of TOC1 in the clock, induction of *LHY* by SA explains the delayed increase in *TOC1* after SA treatment at dawn (Extended Data Fig. 6i, j) when *LHY* has its highest expression. This balanced network architecture of NPR1 regulating both the morning-phased *LHY* and the evening-phased *TOC1* (Fig. 3a) strengthens the clock when the redox rhythm is perturbed.

To investigate the effect of reinforced circadian clock on plant immunity, we examined SA-induced resistance against bacteria in a *toc1* mutant and found it to be more sensitive to induction than wild type and *npr1* (Fig. 4a). While TOC1 negatively regulates resistance against bacteria, CCA1 and LHY have been reported to positively regulate resistance against bacteria and oomycetes[24,25], timing immunity for the morning when temperature and humidity are the most favourable for infection[25]. We hypothesized that SA/NPR1-mediated induction of both morning and evening components of the circadian clock plays a major role in maintaining this diurnal difference in plant sensitivity to pathogen challenge.

To test this, we first examined induction of *WRKY40*, a direct target of TOC1[26], and *PR1*, a direct target of NPR1[27], 3 hours after SA application either in the subjective morning (ZT24) or evening (ZT36) under constant light. Both defence genes had higher induction after the morning treatment (Fig. 4b). We next performed microarray to investigate this time-of-day-specific sensitivity globally (GSE61059) (Patterns of representative genes verified by qPCR shown in Extended Data Fig. 7a, b). We found more genes showing higher induction by morning SA treatment than the evening treatment (like *PR1*) (Fig. 4c). They are mainly defence-related genes (Fig. 4d). In contrast, a larger number of genes appeared to be more repressed after the evening treatment and they are enriched in plant growth and development (Fig. 4d). Furthermore, promoter analysis of the differentially induced genes in the morning showed significant enrichments for both *cis*-elements bound by CCA1/LHY and TOC1, and those of the differentially repressed genes in the evening had significantly enriched *cis*-elements bound by CCA1/LHY (Extended Data Fig. 7c, d). Collectively, these data strongly support our hypothesis that acute perturbation in redox rhythm caused by SA treatment leads to increased expression of both positive and negative regulators of defence, but with the former in the morning and the latter in the evening (Fig. 3a and Extended Data Fig. 7c, d). This may increase the diurnal differences in sensitivity to pathogen challenge in plants.

Gating defence towards the morning may also be a mechanism for plants to minimize interference on growth at night[28,29]. We observed that SA treatment of dark-grown plants could help sustain a more robust circadian rhythm ($P < 10^{-15}$) than mock treatment ($P <$

0.001) (Fig. 4e), but induced a severe loss in fresh weight (Fig. 4f). This is consistent with our hypothesis that untimely induction of immunity at night is detrimental to plant growth. Besides gating immune response, reinforcement of the clock may also help increase photosynthesis and negate the redox perturbation through enhanced expression of *CHLOROPHYLL BINDING PROTEIN 2* (*CAB2*) and evening-phased *CATALASE 3* (*CAT3*) but not the morning-phased *CAT2* (Fig. 4g).

We propose that in *Arabidopsis,* the daily redox rhythm is intrinsically linked with the basal expression of the circadian clock through NPR1 (Fig. 4h and Extended Data Fig. 8). Perturbation in redox rhythms caused by SA during pathogen challenge is sensed by NPR1 to trigger defence gene expression and to reinforce the circadian clock. The wiring of NPR1 to defence genes as well as to the clock shows how plants gate their immune responses towards the morning to anticipate infection while minimizing fitness costs on plant growth which occurs mainly at night[30].

Methods

Plant materials

The *TOC1p:LUC* (Col-0), *LHYp:LUC* (Col-0)[14] and *CAB2p:LUC* (Col-0) seeds were provided by Dr. Robertson McClung and the *toc1-101* mutant[31] by Dr. Shu-Hsing Wu. Mutants of *npr1-3*[18], *sid2*[16], *trx-h3*[19] and *trx-h5*[19] were used to cross with the luciferase reporter lines. *35S:NPR1-GFP* (in *npr1-1*)[12] plants were used in ChIP experiment. To generate *CAT3p:LUC*, *CAT2p:LUC* homozygous lines and different T1 lines of *TOC1p:LUC* and *TOC1p(TBSm):LUC* (*TOC1* promoter with mutated TGA-binding sites), wild-type *CAT3*, *CAT2* and *TOC1* promoters and mutated *TOC1* promoter (amplified using QuikChange Lighting Multi Site-directed mutagenesis kit, Agilent Technologies) were cloned into the pDONR207 vector (Invitrogen) through the Gateway BP reaction (Invitrogen) and then transferred to the destination vector pGWB235[32] through the Gateway LR recombination reaction (Invitrogen). Agrobacterium-mediated transformation of *Arabidopsis* was performed as previously described using wild-type plants[33]. Homozygous T3 lines of *CAT2p:LUC, CAT3p:LUC* and different T1 lines of *TOC1p:LUC* and *TOC1p(TBSm):LUC* were selected and used for the luciferase imaging experiment. All primer sequences used for making the transgenic constructs are listed in Extended Data Table 1.

NADP$^+$ and NADPH measurement

Three-week-old wild-type (Col-0) plants grown in soil under diurnal condition (12 h light/12 h dark) were treated with water or 1 mM SA at subjective dawn and samples were collected every 4 h for two days under constant light conditions. NADP$^+$ and NADPH were measured according to Queval and Noctor[34] with modifications. Briefly, 50 mg of 3-week-old leaves were pulverized in liquid nitrogen using Genogrinder and extracted using 10 mM Tris-HCl (pH 8.0, 1 ml Tris-HCL per 100 mg tissue). The homogenate was centrifuged at 16,000 g for 10 min at 4 °C. The supernatant was separated into two 0.2 ml aliquots. To extract NADP$^+$, 50 μl 1 M HCl was added to one 0.2 ml aliquot. The mixture was heated in boiling water for 1 min. Then 25 μl MES (pH 5.6) was added and the pH of the extract was adjusted to 5–6

using 0.2 M NaOH. To extract NADPH, 50 μl 1 M NaOH was added to the other 0.2 ml aliquot. The mixture was heated in boiling water for 1 min. Then 25 μl MES (pH 5.6) was added and the pH of the extract was adjusted to 7–8 using 0.2 M HCl. Three 20 μl aliquots of the NADP$^+$ and the NADPH extracts were used as technical replicates. Samples containing only the extraction buffer were used as blank. The measurement of the samples and the derivation of the standard curves were performed according to Queval and Noctor[34].

RNA extraction and quantitative PCR

Three-week-old plants grown in soil under diurnal conditions (12 h light/12 h dark) were treated with water or 1 mM SA at subjective dawn and samples were collected every 4 h for two days under constant light conditions. RNA extraction was performed as previously described[18]. cDNA synthesis (SuperScript III, Invitrogen) and quantitative PCR (SYBR Green, Roche) were performed according to the manufacturer's protocols. All primer sequences used for qPCR are listed in Extended Data Table 1.

Luciferase activity measurement

Plants grown in soil with under 12 h light/12 h dark cycles for three weeks were sprayed with 2.5 mM luciferin (Gold Biotechnology) in 0.02% Triton X-100 (Sigma) to activate and deplete pre-existing luciferase due to its instability in the presence of the substrate. Then the plants were transferred into constant light condition. 1 mM SA (Sigma) or water (as control) was sprayed 24 hours later (ZT24). The fifth and sixth leaves were harvested and rinsed three times in 50 ml water. Luciferase was extracted and relative activity was measured according to the manufacturer's protocol (Luciferase Assay System, Promega).

Luciferase imaging

Plants grown in soil under 12 h light/12 h dark cycles for three weeks were sprayed with 2.5 mM luciferin (Gold Biotechnology) in 0.02% Triton X-100 (Sigma) one day before luciferase imaging. Plants were then placed into the imaging system (Nightshade LB985) under either constant light or dark conditions and assayed for bioluminescence by acquiring images with exposure time of 20 min. To test the effect of SA or GSHmee, 1 mM SA (Sigma)/3 mM GSHmee (Sigma) or water (as control) was sprayed at different indicated times. Subsequent quantifications of bioluminescence intensity were performed using Image J.

Analysis of circadian rhythms

The quantified time course bioluminescence data were decomposed into a line and a sine wave with exponentially decaying amplitude:

$Y = Amplitude \times e^{-Kt} \times \sin\left(\frac{2\pi t}{Period} + Phaseshift\right) + a \times t + b$ using GraphPad Prism 6. The intercept of the line at the y-axis ("b") was considered as the average expression level. The period and amplitude were inferred from the sine wave. The exponential decay was used to account for the dampening of bioluminescence over time. The best fitted value, standard error and degrees of freedom were used for statistical analysis.

Western blot

Three-week-old wild-type (Col-0) plants grown in soil under diurnal condition (12 h light/12 h dark) were treated with water or 1 mM SA at subjective dawn and samples were collected every 4 h for two days under constant light. Detection of the NPR1 monomer protein on a non-reducing SDS-PAGE gel was performed as previously described using an antibody against NPR1[12].

Yeast one-hybrid assay

The *TOC1* promoter was first cloned into the pDONR P4-P1R vector (Invitrogen) through the Gateway BP reaction. The entry clones were recombined into destination vectors pMW#2 (Invitrogen) and pMW#3 (Invitrogen). Mutagenesis of the *TOC1* promoter was performed using QuikChange Lighting Multi Site-directed mutagenesis kit (Agilent Technologies) according to the instruction manual. TOC1p_Mut1 (the *TOC1* promoter mutated in the 1st TGA-binding site), TOC1p_Mut2 (the *TOC1* promoter mutated in the 2nd TGA-binding site) and TOC1p_Mut1+2 (the *TOC1* promoter mutated in both TGA-binding sites) were cloned into destination vectors pMW#2 and pMW#3 through the Gateway cloning kit (Invitrogen). The coding sequences of TGAs were cloned into pDONR207 and subsequently transferred into pDEST-AD by the Gateway LR reactions. Transformation of constructs into the yeast strain YM4271 was performed as previously described[35]. Beta-galactosidase reporter activities were measured using ONPG as the substrate[36] and normalized to the control with an empty vector pDEST-AD. All primer sequences used for yeast one-hybrid assay (Y1H) are listed in Extended Data Table 1.

Chromatin immunoprecipitation

Three-week-old soil-grown *35S:NPR1-GFP* (in *npr1-1*)[12] plants were treated with either water (CK) or 1 mM SA at dusk and samples were collected 3 hours after treatment. Chromatin immunoprecipitation (ChIP) was performed as described previously[37]. Immunoprecipitation was performed using a polyclonal antibody against GFP (Ab290, Abcam) and Dynabeads Protein G (Invitrogen). The purified ChIP samples were subject to qPCR using primer pairs for the promoter region (−639 to −589 bp upstream of the start codon) and the coding region (+753 to +803 bp downstream of the start codon) of *TOC1*. Fold of enrichment was calculated using the comparative Ct method[38] using the input samples as normalizers. All primer sequences used for ChIP are listed in Extended Data Table 1.

The mathematical model of the *Arabidopsis* circadian clock

We applied the P2012 plant circadian model from the Plant Systems Modelling portal[13] to elucidate new connections between SA signalling through NPR1 and known plant circadian genes. This numerical ordinary differential equation (ODE) model in MATLAB consists of 32 ODEs and includes transcription terms for 10 genes, which are *LHY/CCA1, PSEUDO-RESPONSE REGULATOR 9, 7, 5* (*PRR9, PRR7, PRR5*), *TOC1, EARLY FLOWERING 4, 3* (*ELF4, ELF3*), *LUX ARRHYTHMO* (*LUX*), *GIGANTEA* (*GI*) and *ABA receptor* (*ABAR*). The 133 parameters in P2012 were previously fitted to multiple datasets in various light-dark photoperiods, different genetic backgrounds, and ABA signalling. It is important to

note that the P2012 model was designed to understand and predict changes in *period* and *phase* when perturbed by genetic or environmental variations. The model does not aim to reflect the exact transcriptional profiles or the absolute protein concentrations.

It was recently shown that plant circadian models exhibit a 'period overshoot' when transitioning from LD to LL cycles[39]. This period overshoot introduced a constant phase delay in the LL data relative to the LD data. Since this phenomenon was not observed in the experimental data, it is an artefact of the mathematical model. For example, the P2012 model predicts that *TOC1* mRNA peaks at ZT18 (i.e., 6 h after subjective light-to-dark transition) under LL conditions[13] instead of the real peak time at ZT12. Moreover, our experiments indirectly measured *TOC1* expression via the luciferase reporter, which is known to exhibit delays[40,41]. This delay was deduced to be 2 h because the luciferase reporter peaked at ZT14 (Fig. 1d) whereas the *TOC1* mRNA peaked at ZT12 (Fig. 1c).

To take this 2-h delay and the 'period overshoot' in the model into consideration, we empirically measured a 4-h delay between simulation *TOC1* mRNA levels and our luminescence data. This total 4-h delay was inferred by aligning the second peak after the LD to LL transition in our luciferase experiments (38 h) and *TOC1* mRNA in the model (42 h). We subsequently used this 4-h delay to correctly align and fit the P2012 simulation *TOC1* mRNA to our experimental luciferase data.

Addition of NPR1 regulation to the circadian clock model

While keeping the original P2012 parameters fixed, we added NPR1 as a transcriptional activator of *TOC1,* as it has been shown experimentally. We also added NPR1 as a transcriptional activator of two additional clock genes ("query pair"). Our goal was to systematically determine which query pair best fitted our measured *TOC1p:LUC* expression in wild type and *npr1-3* in mock- and SA-treated plants. We multiplied the P2012 transcriptional synthesis term of *TOC1* and each gene in the query pair by their own NPR1-dependent regulatory function F(t) (i.e., non-competitive activation). Each regulatory function F has the form:

$$F(t) = n_b + n_a \frac{[NPR1(t)]}{[NPR1(t)] + K_d}$$

where [NPR1(t)] is the NPR1 monomer concentration over time, n_b is the basal, NPR1-independent transcription level of the gene of interest, n_a is the maximum NPR1-activated transcription level of the gene and K_d is the effective DNA-binding dissociation constant for the gene. The [NPR1(t)] monomer levels for mock-treated and SA-treated plants were taken from western blot data in Fig. 2b and Extended Data Fig. 4. The NPR1 data for the mock-treated and SA-treated plants were then averaged, normalized, and linearly interpolated to serve as an input function for modelling (Extended Data Fig. 9a, b).

Least squares fitting of the *TOC1p:LUC* data

For every query pair and the *TOC1* gene, we optimized n_b, n_a, K_d parameters (among the 9 parameters, 6 are independent; see below) to give the best least squares fit of the *TOC1*

mRNA in the model to the patterns of *TOC1p:LUC* expression in wild-type and *npr1-3* with mock- or SA-treated plants over several circadian cycles (Fig. 2a).

Because the time of sampling and the waveforms were different between our experiments and the P2012 model, our luciferase data could not be fitted directly to the model. To solve the sampling time discrepancy, data points from our experiments and the P2012 datasets were interpolated (via cubic spline) to a time resolution of 0.1 h. To circumvent the waveform issue, we first calculated the ratio (R) of *npr1-3/*WT and SA-treated/mock-treated WT in experimental *TOC1p:LUC* data:

$$R_{npr1}(t) = \frac{TOC1_{npr1}(t)}{TOC1_{WT}(t)}, R_{SA}(t) = \frac{TOC1_{SA}(t)}{TOC1_{WT}(t)},$$

where $TOC1_{WT}$, $TOC1_{npr1}$ and $TOC1_{SA}$ are interpolated experimental data for *TOC1p:LUC* in (1) mock-treated wild type, (2) mock-treated *npr1* mutant, (3) SA-treated wild type, respectively. We then created target P2012 simulation of $TOC1_{npr1}$ or $TOC1_{SA}$ mRNA data by multiplying the $TOC1_{WT}$ mRNA data in the simulation by R_{npr1} or R_{SA}. We optimized the regulatory function parameters (n_b, n_a, K_d) for each combination of query genes and *TOC1*. The parameter optimization used nonlinear least squares fitting to minimize the sum of squared residual of *TOC1* expression (i.e., squared difference between the model and the target *TOC1* mRNA profile). To account for the 4-h delay inherent to 'period-overshoot' in the P2012 model and the use of the reporter, we started fitting at 28 h, which corresponds to 24 h in our experiments. We fitted 3-day-long *npr1-3* mutant data and 2-day-long WT and SA treatment data.

Fitting of the *npr1-3* mutant data

For the first part of the fitting process, we set [NPR1] = 0, which resulted in a single parameter (n_b) fit for each candidate gene. Because we coupled NPR1-activation to *TOC1* and two other query genes, 3 parameters in total were fitted for each query pair. The optimal parameters n_b^* were restricted to a value between 0 and 1, where 0 represents no transcription in absence of NPR1 and 1 represents the absence of any regulation by NPR1. We used the function fmincon in MATLAB (2013b, MathWorks, Natick, MA, USA) with sequential programming algorithm without restrictions. We found the 3 parameters that minimized the least squares residual of TOC1 model output to target P2012 $TOC1_{npr1}$ data. Because nonlinear least squares fitting uses a deterministic algorithm that can become trapped in a local minimum, we ran the simulations from 15 different random starting points to find the global minimum. We confirmed that nonlinear least squares fitting of most query pairs converged to the same global minimum when started from random parameters (Extended Data Fig. 9c, d).

A plot of the best least squares fit for each query gene showed a cross-hair pattern centred on *PRR7* in Fig. 3b. The *npr1* data (reduced *TOC1* amplitude, no change in phase or period) are mostly explained by including *PRR7* as an additional target of NPR1 regulation (Extended Data Fig. 6a, b), such that *PRR7* levels are reduced in the *npr1* mutant (Fig. 3c).

A role for NPR1 in regulating basal expression of *PRR7* is consistent with previous genetic data showing that lowering *TOC1* expression shortens the circadian period[23], whereas lowering *PRR7* expression lengthens the circadian period[42]. Analytical work has previously shown how mutations in opposing components in the clock can lead to unchanged period[43]. We used our best-fit P2012 model to verify that lowered *PRR7* expression lengthens the period by ~2 h, whereas lowered *TOC1* expression shortens the period by ~2 h in *npr1*. Thus, the simultaneous, balanced reduction in expression of two opposing nodes (i.e., *TOC1* and *PRR7*) explains why the period of *TOC1p:LUC* expression is not altered in *npr1*.

Mock-treated WT data constrain the parameters

During our fitting procedure for mock-treated WT data, we discovered that optimal n_a^*, K_d^* always exhibited a simple relationship (Extended Data Fig. 9e). The constraint that explains this empirical relationship is that our final choice of n_a^*, K_d^* should not alter clock expression in mock-treated WT. Mathematically, n_a^*, K_d^* should have no effect, *on average*, on gene expression in mock-treated WT. This condition restricts n_a^* to depend on K_d^* because the time-averaged $<[NPR1]>$ in WT is normalized to 1, such that

$$<F> \approx n_b^* + n_a^* \frac{<[NPR1]>}{<[NPR1]> + K_d^*} = n_b^* + n_a^* \frac{1}{1 + K_d^*} = 1$$

Thus, we recovered the simple empirical relationship observed in Extended Data Fig. 9e as

$$n_a^* = (1 - n_b^*)(1 + K_d^*)$$

Fitting of the SA treatment data

By using the best-fit value for n_b^* from Step 1 and the constraint from Step 2 to fix n_a^*, we only needed to fit a single parameter (k_d). We restricted k_d to lie between 0 (i.e., always maximum expression, insensitive to SA treatment and NPR1 monomer levels) and 5. We verified that allowing k_d to be as high as 50 did not significantly improve the least squares fit. For each query pair, we ran nonlinear least squares fit from 15 random starting points. We found that again, in general, they converged to the same global optimum (Extended Data Fig. 9f, g). Fig. 3d shows a cross-hair pattern centred on *LHY/CCA1* suggesting that *LHY/CCA1* activation by the induced, arrhythmic NPR1 levels during SA treatment should counteract the effect of *TOC1* induction. We noted that the best-fit solution from a *TOC1*-only case shows immediate *TOC1* induction after SA treatment (Extended Data Fig. 6i) instead of the observed delay until dusk. However, if we added *LHY* as an NPR1 target in addition to *TOC1*, the modelling results best fit our experimental data (Extended Data Fig. 6j). Consistently, *LHY* expression was found to be induced by SA (Fig. 3e), but reduced in the *npr1* mutant (Extended Data Fig. 6g).

Limitations of the model

There are limitations to our model. First, our model was only fitted to the expression of one gene (*TOC1p:LUC*) under 3 conditions (i.e., wild-type with and without SA treatment, and *npr1*). Second, our model combines *LHY/CCA1* into one gene and cannot resolve the experimental differences that we observed in those genes (Fig. 3e and Extended Data Fig. 6c, d). Third, our model for the SA-induction data pre-sets *PRR7* at maximum expression even without SA treatment (i.e., $K_d = 0$) (Extended Data Fig. 9g). This is unlikely an accurate reflection of a real physiological state. Last, all our experiments and modelling were done under constant light conditions and the additive (acute) light activation terms are effectively 0 because the hypothetical protein responsible for light activation has decayed to 0. These additive light terms should not be affected by our assumption of non-competitive activation by NPR1. Uncovering the proper relationship between the light-dependent terms and the NPR1-dependent terms (i.e., competitive versus non-competitive activation) would require experiments under diurnal conditions. This is outside of the scope of the current paper.

Even though the modelling approach correctly predicted *PRR7* and *LHY* as direct targets of NPR1, it had mixed results with *ELF3*, which is not a direct target. Our model predicted *ELF3* to decrease after SA treatment and to increase in the *npr1* mutant. The lack of induction in *ELF3* by SA (Extended Data Fig. 6e) was consistent with the model prediction. However, the significantly decreased expression of *ELF3* observed in *npr1* (Extended Data Fig. 6h) was not in agreement with the model. This discrepancy suggests there are other links between NPR1 and the circadian clock that the current model cannot capture. A future model should be fitted to *ELF3p:LUC*, which would be an informative constraint.

Bacterial infection

Three-week-old plants grown in soil were pre-treated with water or 1 mM SA at ZT12 and infiltrated 24 hours later with *Pseudomonas syringae* pv. *maculicola* (*Psm*) ES4326 ($OD_{600nm} = 0.001$) as previously described[12]. Briefly, 8 plants/genotype/treatment were inoculated with *Psm* ES4326 and bacterial growth was measured 3 days post inoculation.

Microarray analysis

To test time-of-day-specific sensitivity to SA, 3-week-old soil-grown plants were transferred to constant light condition one day before treatment. Water or 1 mM SA were applied in the subjective morning (ZT24) or evening (ZT36). The fifth and sixth leaves were sampled 0 and 3 hours after treatment. RNA was extracted, amplified, labelled and hybridised to ATH1 GeneChip (Affymetrix) as previously reported[25]. The arrays were normalized with RMA algorithm and centred to median. Two-way ANOVA ($P < 0.05$) and Student's *t*-test with multiple comparison correction ($P < 0.05$, Fold changes > 2) were used to identify genes that were significantly more induced or more repressed by water or SA when treated at ZT24 or at ZT36. Athena program (http://www.bioinformatics2.wsu.edu/Athena) was used to identify *cis*-elements bound by CCA1/LHY including evening element, CCA1-binding site, CCA1 motif1 BS in CAB1 and CCA1 motif2 BS in CAB1. Hypergeometric distribution was used to determine statistical significance. Enriched gene ontology

categories were identified using BiNGO (http://www.psb.ugent.be/cbd/papers/BiNGO/ Home.html).

Fresh/dry weight measurement

Three-week-old soil-grown wild-type (Col-0) plants were transferred into constant dark condition or normal diurnal condition at dusk. After 36 h, water (control) or 1 mM SA was applied. Two days after treatment, pictures were taken and fresh/dry weight was measured.

Statistical analysis

Statistical analysis was performed using GraphPad Prism 6 (GraphPad Software). All the centre values shown in the figures are means of technical (Figs. 1a, 1b, 2d and Extended Data Fig. 1) or biological (all other figures where applicable) replicates. Experiments were repeated twice for Figs. 1a, 1b and *CAB2p:LUC* in 4g. All other experiments were repeated three times where applicable. Harmonic regression ($Y = a\sin\frac{\pi t}{12} + b\cos\frac{\pi t}{12} + c$) followed by ANOVA test was used to identify statistically significant oscillation. The null hypothesis is that all data across different time points are sampled from the same normal distribution. Student's *t*-test with multiple comparison correction was performed to identify statistically significant differences between mock and treated samples. Two-way ANOVA was used to assess significant interactions between genotype and treatment or between time of treatment and treatment. Significant interactions suggest the effect of the treatment is dependent on genotype or time of treatment. Tukey's multiple comparisons test was performed to identify the orders of samples that are significantly different from each other. All statistical tests are two-sided tests where applicable.
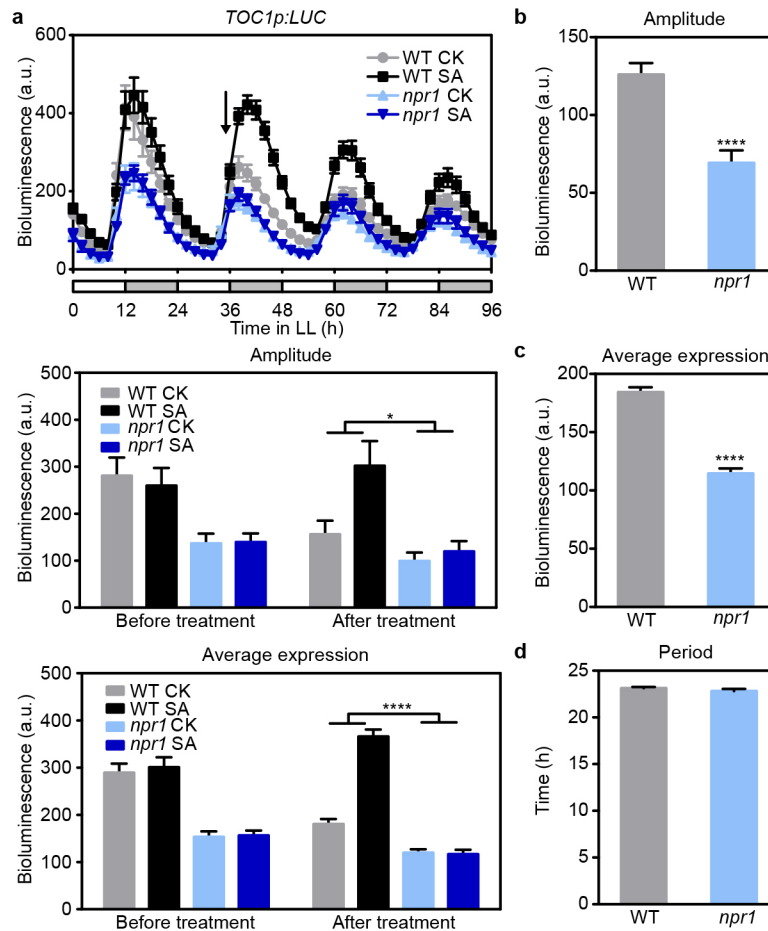
Extended Data
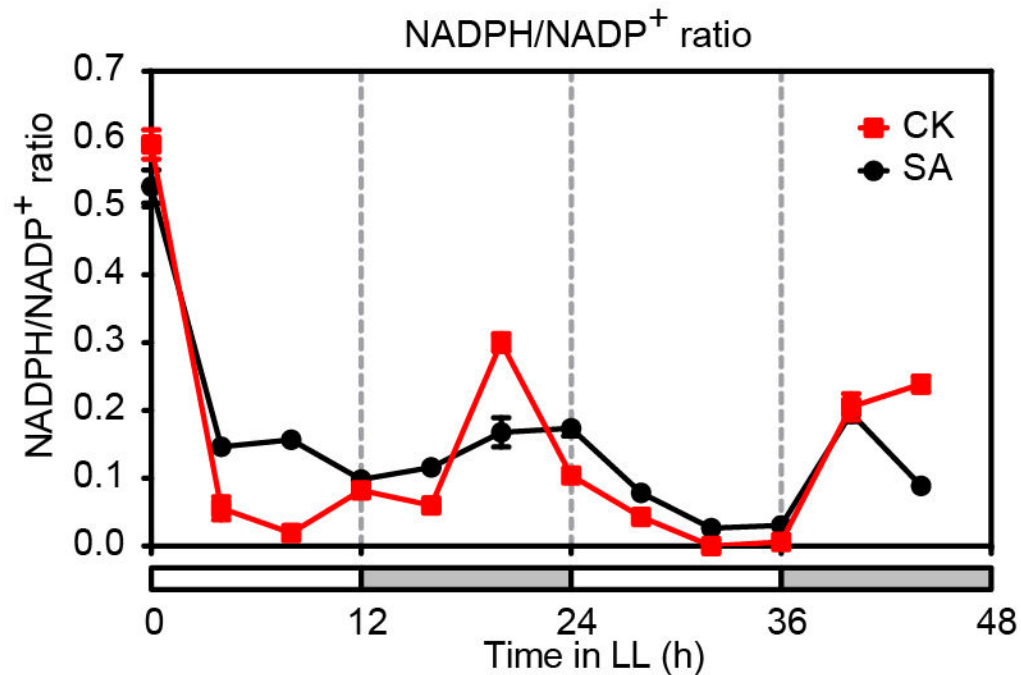
Extended Data Figure 1. Circadian oscillation of the NAPDH/NADP$^+$ ratio

NADPH/NADP$^+$ ratios in 3-week-old soil-grown plants derived from Fig, 1a, b. Water (CK) or 1 mM SA was applied at 0 h. Data are mean ± s.e.m. (n = 3). White bars represent subjective days and grey bars represent subjective nights. Harmonic regression analysis suggests significant circadian oscillation of water-treated NADPH/NADP$^+$ ratio (P < 0.0001).
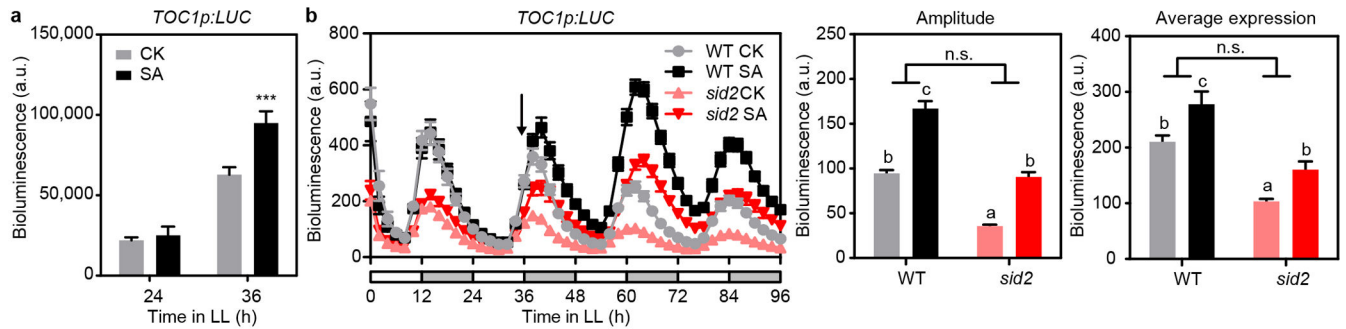

Extended Data Figure 2. The effects of exogenous and endogenous SA on *TOC1* expression

a, Luciferase activity measurements using the *TOC1p:LUC* plant extracts. Relative luciferase activity of the fifth and sixth leaves from 3-week-old soil-grown *TOC1p:LUC* plants. Water (CK) or 1 mM SA was applied at ZT24. LL, constant light. a.u., arbitrary unit. Data are mean ± s.e.m. (n = 6 biological replicates; *t*-test; ***, P < 0.001). **b,** *TOC1p:LUC* activity rhythms in 3-week-old soil-grown wild-type (WT) and *sid2* plants treated with water (CK) or 1 mM SA at subjective dusk (black arrow) (mean ± s.e.m., n = 8 plants). White bars represent subjective days and grey bars represent subjective nights. The bar graphs represent the estimates of amplitude and average expression of *TOC1p:LUC*, respectively (mean ± s.e.m.). The letters above the bars indicate statistically significant differences between groups at P < 0.05 (Tukey's multiple comparisons test). n.s., non-significant (two-way ANOVA, non-significant interaction between genotype and treatment). This experiment has been repeated three times with similar results.
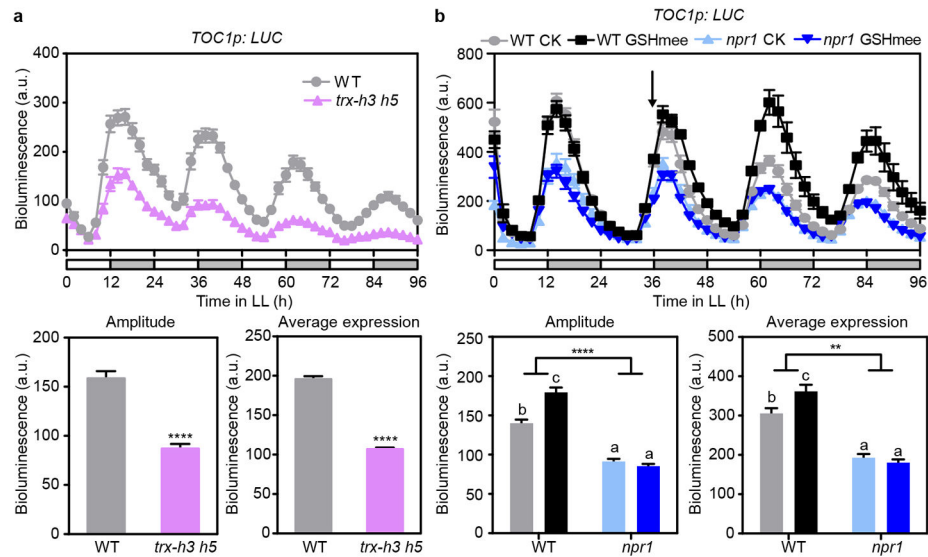
Extended Data Figure 3. NPR1 regulates the amplitude and average expression of *TOC1p:LUC*
a, *TOC1p:LUC* activity rhythms in 3-week-old soil-grown wild-type (WT) and *npr1-3*
plants treated with water (CK) or 1 mM SA at subjective dusk (black arrow) (mean ± s.e.m.;
n = 6 plants). LL, constant light. a.u., arbitrary unit. White bars represent subjective days
and grey bars represent subjective nights. The bar graphs show the estimates of amplitude
and average expression level (mean ± s.e.m.; two-way ANOVA; *, $P < 0.05$; ****, $P <
0.0001$). **b–d,** Estimates of amplitude (**b**), average expression (**c**) and period (**d**) of
TOC1p:LUC in wild-type (WT) and *npr1-3*. Data are mean ± s.e.m. (*t*-test; ****, $P <
0.0001$). These experiments have been repeated three times with similar results.
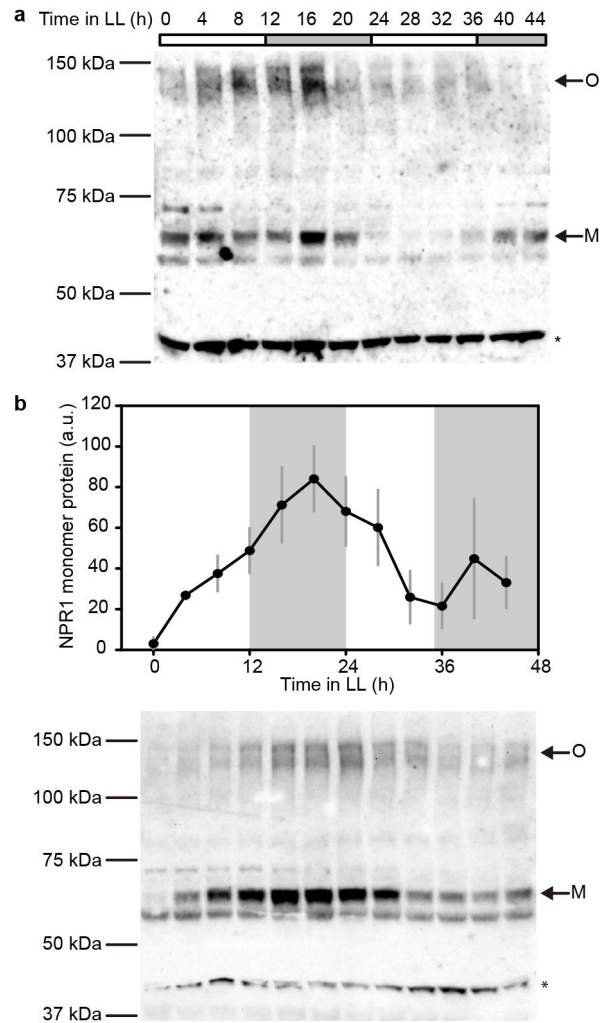
Extended Data Figure 4. The abundance of NPR1 monomer under constant light conditions
NPR1 monomer (M) abundance in 3-week-old soil-grown plants without treatment (**a**) and after 1 mM SA treatment at 0 h (**b**) under constant light (LL) conditions. NPR1 protein were detected using western blot after non-reducing SDS-PAGE (**a, b**). NPR1 monomer protein was quantified using the non-specific band (*) as a loading control (**b**; mean ± s.e.m.; $n = 3$ biological replicates; a.u., arbitrary unit). O, NPR1 oligomer. White bars represent subjective days and grey bars represent subjective nights.

Extended Data Figure 5. Redox perturbations affect the amplitude and average expression of *TOC1p:LUC* in an NPR1-dependent manner

a, *TOC1p:LUC* activity rhythms in 3-week-old soil-grown wild-type (WT) and *trx-h3 trx-h5* (*trx-h3 h5*) (mean ± s.e.m., *n* = 6 plants). LL, constant light. a.u., arbitrary unit. White bars represent subjective days and grey bars represent subjective nights. The bar graphs show the estimates of amplitude and average expression (mean ± s.e.m.; *t*-test; ****, *P* < 0.0001). **b,** *TOC1p:LUC* activity rhythms in 3-week-old soil-grown wild-type (WT) and *npr1* plants treated with water (CK) or 3 mM GSHmee at subjective dusk (black arrow) (mean ± s.e.m., *n* = 8 plants). The bar graphs represent the estimates of amplitude and average expression of *TOC1p:LUC,* respectively (mean ± s.e.m.). The letters above the bars indicate statistically significant differences between groups at *P* < 0.01 (Tukey's multiple comparisons test). **, *P* < 0.01; ****, *P* < 0.0001 (two-way ANOVA). These experiments have been repeated three times with similar results.
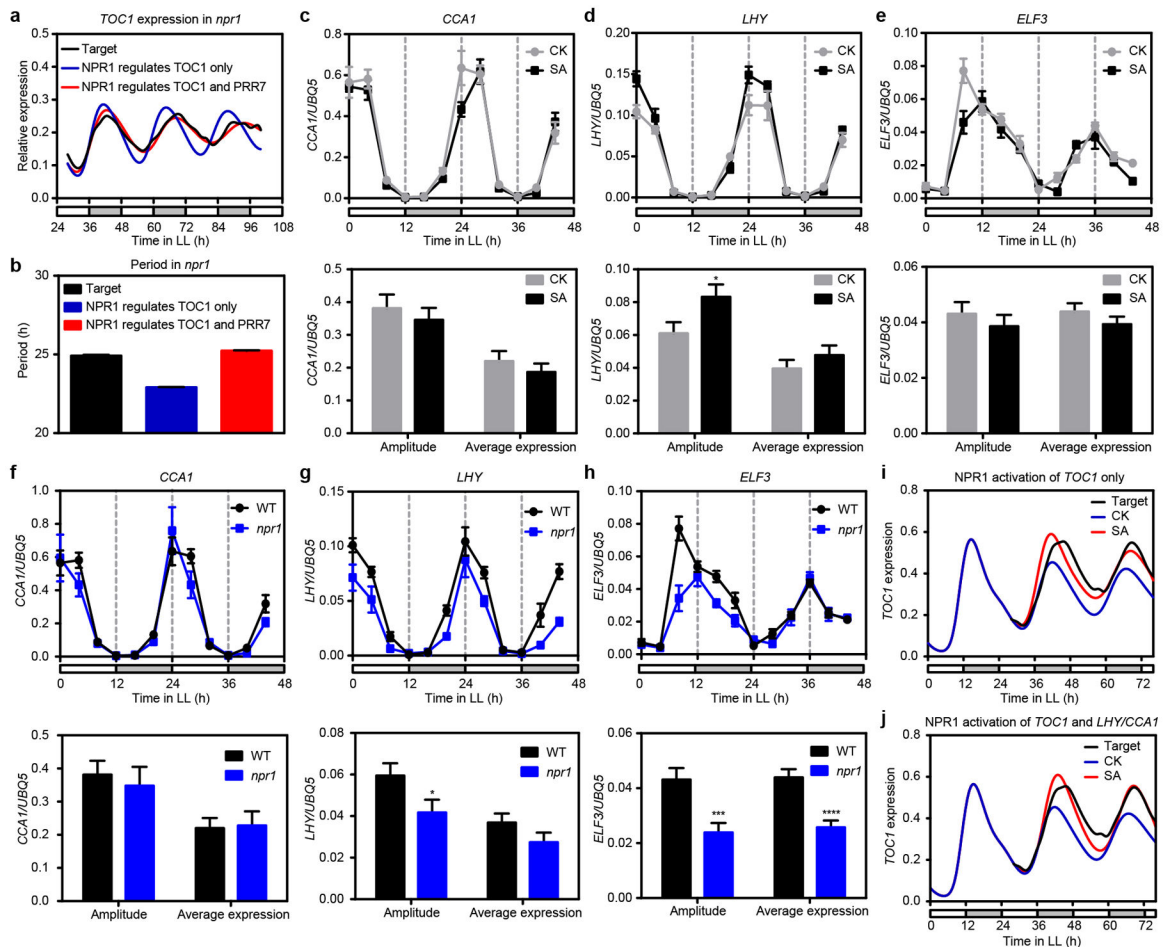
**Extended Data Figure 6. Model prediction and validation**

a, Comparison of best-fit solutions for the TOC1-only and the TOC1-and-PRR7 coupling in *npr1*. LL, constant light. White bars represent subjective days and grey bars represent subjective nights. **b,** Addition of PRR7 coupling improves the fitness and mostly rescues the short period phenotype of the TOC1-only model (mean ± s.e.m.; *n* = 715, *n* is degree of freedom derived from nonlinear regression). **c–e,** The transcript levels of *CCA1* (**c**), *LHY* (**d**) and *ELF3* (**e**) in wild-type plants after water (CK) or 1 mM SA treatment. **f–h,** The transcript levels of *CCA1* (**f**), *LHY* (**g**) and *ELF3* (**h**) in wild-type (WT) and *npr1* plants. The expression was normalized to *UBQ5* (**c–h**). The bar graphs show the estimates of amplitude and average expression level, respectively (**c–h**; mean ± s.e.m.; *n* = 3 biological replicates; *t*-test; *, $P < 0.05$; ***, $P < 0.001$; ****, $P < 0.0001$). **i, j,** Comparison of best-fit solutions for NPR1 activation of *TOC1*-only (**i**) and NPR1 activation of *TOC1* and *LHY/CCA1* (**j**) after SA treatment.
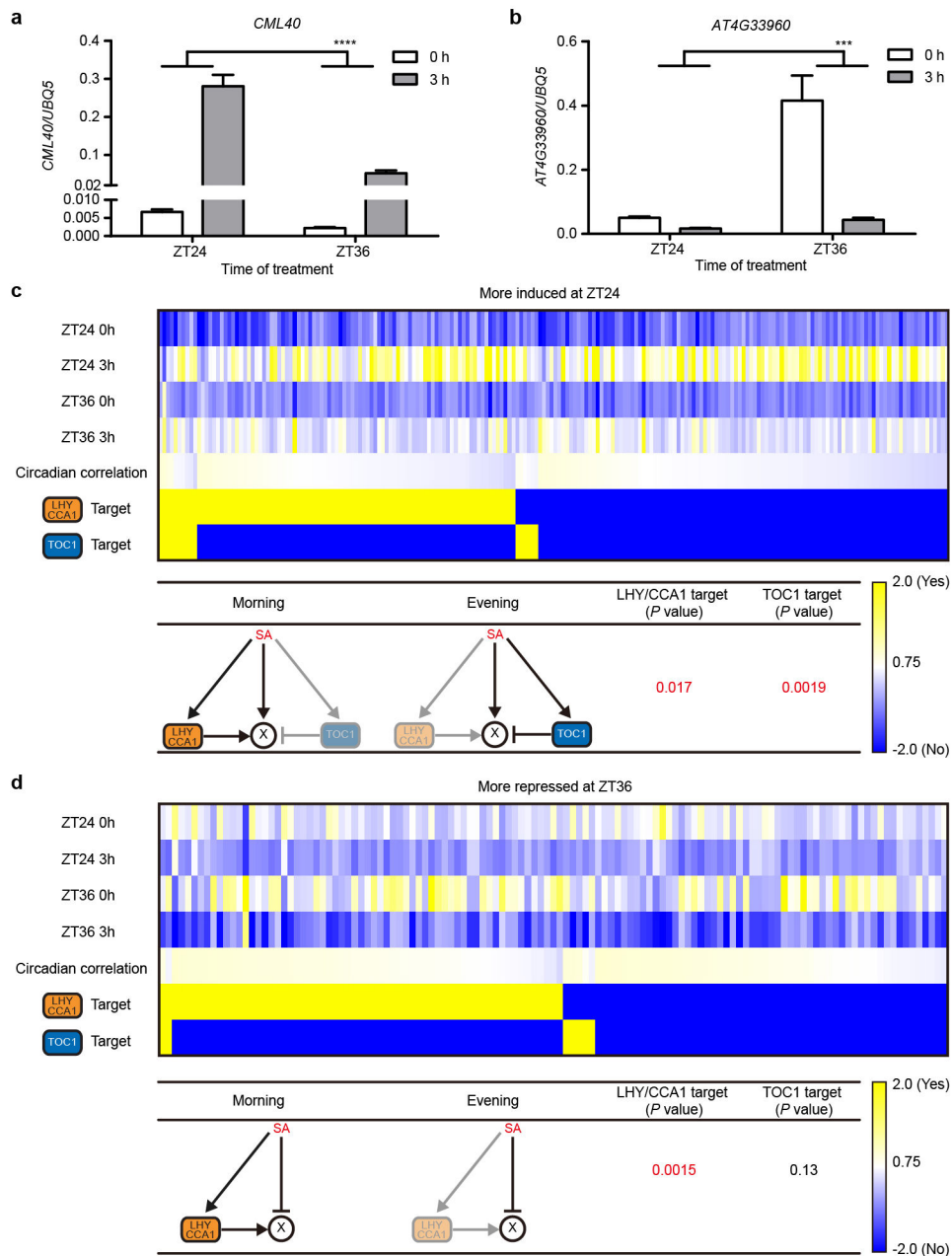
**Extended Data Figure 7. Validation and analysis of microarray data**

a, b, The transcript levels of *CML40* (**a**) and *AT4G33960* (**b**) in 3-week-old soil-grown plants 0 or 3 hours (h) after application of 1 mM SA either in the subjective morning (ZT24) or in the subjective evening (ZT36) normalized to *UBQ5* under constant light conditions. Data are mean ± s.e.m. ($n = 3$ biological replicates; two-way ANOVA; ***, $P < 0.001$; ****, $P < 0.0001$). **c, d,** Enrichment of *cis*-elements affecting time-of-day-specific sensitivity to induction. Promoter analysis of genes that were more induced by SA when treated at ZT24 (**c**) or more repressed by SA when treated at ZT36 (**d**). The heat maps show the average expression levels based on the microarray. Circadian correlation coefficients were extracted from Diurnal (http://diurnal.mocklerlab.org/diurnal_data_finders/new).

Yellow represents a high value or a target of CCA1/LHY or TOC1. Blue represents low a value or not a target of CCA1/LHY or TOC1. 'X' represents a gene that was more induced by SA when treated at ZT24 (**c**) or more repressed by SA when treated at ZT36 (**d**). Arrows represent activation. Block arrows represent repression. *P* values were determined based on hypergeometric distribution.
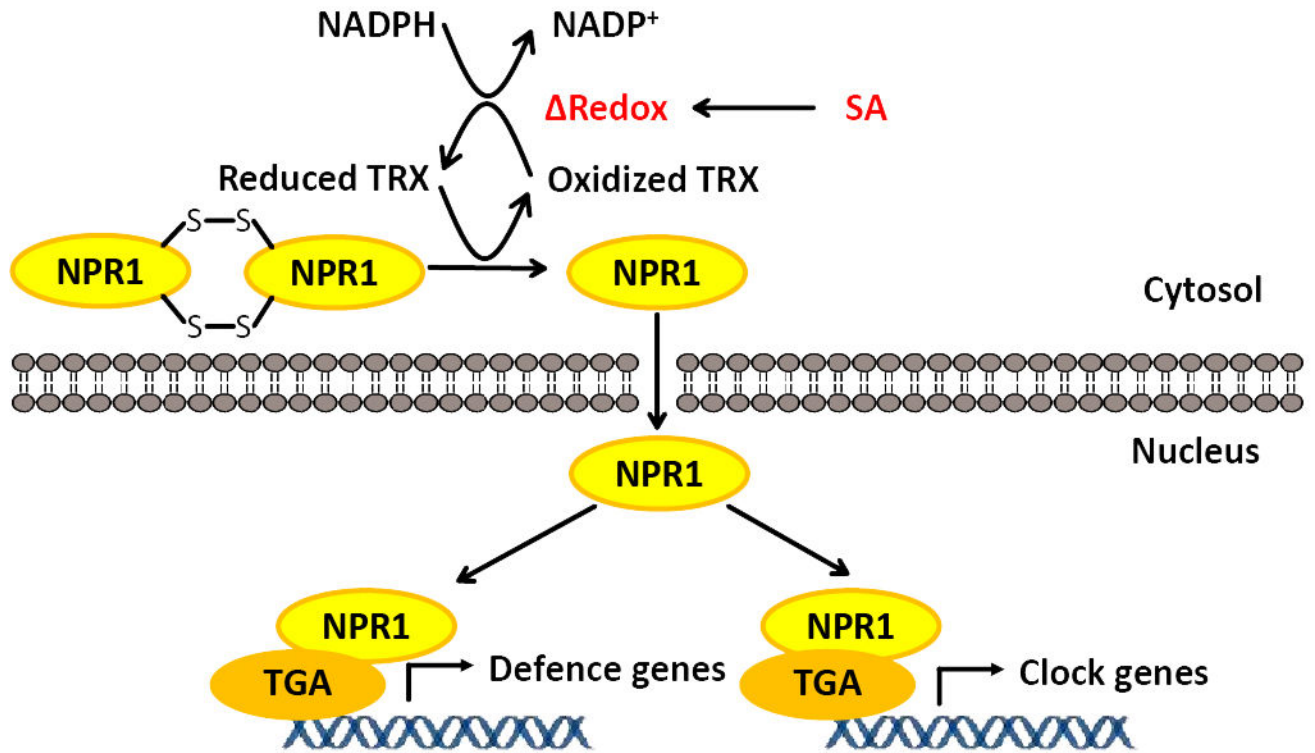
Extended Data Figure 8. NPR1 senses and transduces redox signals to trigger transcriptional reprogramming

SA-triggered redox changes induce the oligomer-to-monomer switch of NPR1. The monomer then enters the nucleus and up-regulates both defence genes and clock genes through interaction with TGA TFs.
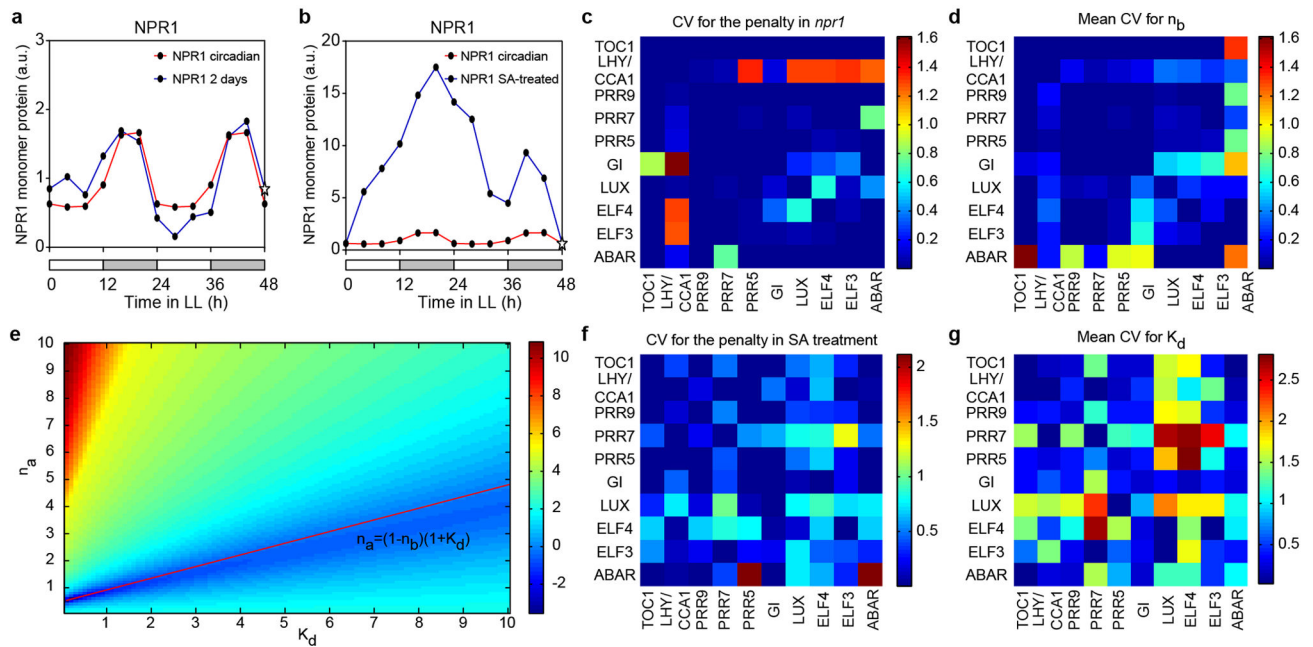
Extended Data Figure 9. Technical details for model fitting

a, Normalized NPR1 monomer abundance in mock-treated samples. The blue line presents the mean values from Fig. 2b, where the value at 48 h (marked with an open star) was inferred to be the same as 0 h. The red line represents the smoothened values used for modelling by averaging over two days to create a one-day trace, which was then repeated over two days. The smoothened data were normalized, such that the time average of NPR1 was equal to 1. LL, constant light. a.u., arbitrary unit. White bars represent subjective days and grey bars represent subjective nights. **b,** SA-treated NPR1 monomer abundance. NPR1 monomer abundance after SA treatment from Extended Data Fig. 4b was normalized so that 0 h has the same value as the corresponding mock-treated NPR1 monomer level. Based on the assumption that the SA induction lasted for two days, the value of the last time point was inferred to be equal to the basal level (marked with an open star). **c,** Coefficient of variation (CV) of least squares residual Σ for 15 different, random initial parameters for the model fitting of *npr1* data. **d,** CV of n_b^* for 15 different, random initial parameters for the model fitting of *npr1* data. **e,** Optimal n_a^*, K_d^* exhibit a linear relationship. $\log(\Sigma)$ was plotted as a function of n_a and K_d for mock-treated TOC1-only coupling (no query pairs). A "low", linear Σ region is evident and is described by a simple analytical linear relationship. $n_b^* = 0.5689\ h^{-1}$. **f,** CV of Σ for 15 different, random initial parameters for the model fitting of SA-treated data. **g,** The CV of K_d^* for 15 different, random initial parameters for the model fitting of SA-treated data.

Extended Data Table 1

Primer sequences

Purpose	Primer name	Sequences
Transgenic plants	TOC1p_F	GGGGACAAGTTTGTACAAAAAAGCAGGCTTAGAGATCGCTCGGCTCAACAA

| Purpose	Primer name	Sequences
	TOC1p_R	GGGGACCACTTTGTACAAGAAAGCTGGGTCATTGTTTTGTTTTGTCAATC
	TOC1p_Mut1	ATATTTTCTCCAAGAGTCCGTGGCCTTTTCTC
	TOC1p_Mut2	TTTTTATTGTCCACGGACTCTCCTTGGCCTAA
	CAT3p_F	GGGGACAAGTTTGTACAAAAAAGCAGGCTTACCCAAAGCTTCTGGCATTTTTTGACTTTTGTCG
	CAT3p_R	GGGGACCACTTTGTACAAGAAAGCTGGGTAGGTGATGATAGAAGGTTGATGATCCCCCAAATAGGCTT
	CAT2p_F	GGGGACAAGTTTGTACAAAAAAGCAGGCTTACAAGTAATCGATCATCCTTAAGTTTGGT
	CAT2p_R	GGGGACCACTTTGTACAAGAAAGCTGGGTAGGTTTGATGAGAAGAGAGCTTGGAGAGA
	TOC1p_P4P1R_F	GGGGACAACTTTGTATAGAAAAGTTGGAGATCGCTCGGCTCAACAA
	TOC1p_P4P1R_R	GGGGACTGCTTTTTTGTACAAACTTGATTGTTTTGTTTTGTCAATC
	TOC1p_Mut1	ATATTTTCTCCAAGAGTCCGTGGCCTTTTCTC
	TOC1p_Mut2	TTTTTATTGTCCACGGACTCTCCTTGGCCTAA
	TGA1_F	GGGGACAAGTTTGTACAAAAAAGCAGGCTTAATGAATTCGACATCGACACAT
	TGA1_R	GGGGACCACTTTGTACAAGAAAGCTGGGTCCGTTGGTTCACGATGTCGAGT
	TGA2_F	GGGGACAAGTTTGTACAAAAAAGCAGGCTTAATGGCTGATACCAGTCCGAGA
	TGA2_R	GGGGACCACTTTGTACAAGAAAGCTGGGTCCTCTCTGGGTCGAGCAAGCCA
Y1H	TGA3_F	GGGGACAAGTTTGTACAAAAAAGCAGGCTTAATGGAGATGATGAGCTCTTCT
	TGA3_R	GGGGACCACTTTGTACAAGAAAGCTGGGTCAGTGTGTTCTCGTGGACGAGC
	TGA4_F	GGGGACAAGTTTGTACAAAAAAGCAGGCTTAATGAATACAACCTCGACACAT
	TGA4_R	GGGGACCACTTTGTACAAGAAAGCTGGGTCCGTTGGTTCACGTTGCCTAGC
	TGA5_F	GGGGACAAGTTTGTACAAAAAAGCAGGCTTAATGGGGAGATACTAGTCCAAGA
	TGA5_R	GGGGACCACTTTGTACAAGAAAGCTGGGTCCTCTCTTGGTCTGGCAAGCCA
	TGA6_F	GGGGACAAGTTTGTACAAAAAAGCAGGCTTAATGGCTGATACCAGTTCAAGG
	TGA6_R	GGGGACCACTTTGTACAAGAAAGCTGGGTCCTCTCTTGGCCGGGCAAGCCA
	TGA7_F	GGGGACAAGTTTGTACAAAAAAGCAGGCTTAATGATGAGTTCTTCTTCTCCA
	TGA7_R	GGGGACCACTTTGTACAAGAAAGCTGGGTCAGTTGGTTCTTGTGGACGAGC
	TOC1_qP_F	AATAGTAATCCAGCGCAATTTTCTTC
	TOC1_qP_R	CTTCAATCTACTTTTCTTCGGTGCT
	LHY_qP_F	CGCTGCTTCGGTCTGGCCTT
	LHY_qP_R	TGTAGCAGCGGCAATGGCAGT
	PRR7_qP_F	CAGTCCACGAGCGGTATCTC
	PRR7_qP_R	CCAGGGCCAGATCACAGTTT
	CCA1_qP_F	TGACCGGTCCTCGTGTGGCT
	CCA1_qP_R	ACTGCGGCGTGCATTGGACT
	ELF3_qP_F	TGGCAAAACTCGTCTGAAGGA
	ELF3_qP_R	GCCAAGTGAGATTCAGCTCCAT
qPCR	PR1_qP_F	CTCATACACTCTGGTGGG
	PR1_qP_R	TTGGCACATCCGAGTC
	WRKY40_qP_F	ACAACGTCTTGAGGAAGCAAC
	WRKY40_qP_R	TCCGTTGAGCTACTCTCCGA
	CML40_qP_F	GAGCCACCAAGGCAAGGTAT
	CML40_qP_R	GTCCTCGAGCTCCAACGATT
	AT4G33960_qP_F	CGTCCAGATTGTTATGCGGC
	AT4G33960_qP_R	TGGAGAAGGGTAAGAAGCGG
	UBQ5_qP_F	GACGCTTCATCTCGTCC
	UBQ5_qP_R	GTAAACGTAGGTGAGTCC
	TOC1 ChIP promoter_F	TGTCCACGTCATCTCCTTGG
ChIP	TOC1 ChIP promoter_R	AGCTTAATGGTGGGACTTGGG
	TOC1 ChIP coding region_F	GAGGCAAGACGAAGTCCCTG
	TOC1 ChIP coding region_R	GCTGCACCTAGCTTCAAGCA

Author Manuscript

Author Manuscript

Author Manuscript

Author Manuscript

Acknowledgments

References

1. O'Neill JS, et al. Circadian rhythms persist without transcription in a eukaryote. Nature. 2011; 469:554–558. [PubMed: 21270895]

2. O'Neill JS, Reddy AB. Circadian clocks in human red blood cells. Nature. 2011; 469:498–503. [PubMed: 21270888]

3. Edgar RS, et al. Peroxiredoxins are conserved markers of circadian rhythms. Nature. 2012; 485:459–464. [PubMed: 22622569]

4. Peek CB, et al. Circadian clock NAD+ cycle drives mitochondrial oxidative metabolism in mice. Science. 2013; 342:1243417. [PubMed: 24051248]

5. Ramsey KM, et al. Circadian clock feedback cycle through NAMPT-mediated NAD+ biosynthesis. Science. 2009; 324:651–654. [PubMed: 19299583]

6. O'Neill JS, Maywood ES, Chesham JE, Takahashi JS, Hastings MH. cAMP-dependent signaling as a core component of the mammalian circadian pacemaker. Science. 2008; 320:949–953. [PubMed: 18487196]

7. Lai AG, et al. CIRCADIAN CLOCK-ASSOCIATED 1 regulates ROS homeostasis and oxidative stress responses. Proceedings of the National Academy of Sciences of the United States of America. 2012; 109:17129–17134. [PubMed: 23027948]

8. McClung CR. The genetics of plant clocks. Advances in genetics. 2011; 74:105–139. [PubMed: 21924976]

9. Nagel DH, Kay SA. Complexity in the wiring and regulation of plant circadian networks. Current biology : CB. 2012; 22:R648–657. [PubMed: 22917516]

10. Pokhilko A, et al. The clock gene circuit in Arabidopsis includes a repressilator with additional feedback loops. Molecular systems biology. 2012; 8:574. [PubMed: 22395476]

11. Zhong HH, McClung CR. The circadian clock gates expression of two Arabidopsis catalase genes to distinct and opposite circadian phases. Molecular & general genetics : MGG. 1996; 251:196–203. [PubMed: 8668130]

12. Mou Z, Fan W, Dong X. Inducers of plant systemic acquired resistance regulate NPR1 function through redox changes. Cell. 2003; 113:935–944. [PubMed: 12837250]

13. Pokhilko A, Mas P, Millar AJ. Modelling the widespread effects of TOC1 signalling on the plant circadian clock and its outputs. BMC systems biology. 2013; 7:23. [PubMed: 23506153]

14. Kim WY, Salome PA, Fujiwara S, Somers DE, McClung CR. Characterization of Pseudo-Response Regulators in Plants. Method Enzymol. 2010; 471:357–378.

15. Goodspeed D, Chehab EW, Min-Venditti A, Braam J, Covington MF. Arabidopsis synchronizes jasmonate-mediated defense with insect circadian behavior. Proceedings of the National Academy of Sciences of the United States of America. 2012; 109:4674–4677. [PubMed: 22331878]

16. Nawrath C, Metraux JP. Salicylic acid induction-deficient mutants of Arabidopsis express PR-2 and PR-5 and accumulate high levels of camalexin after pathogen inoculation. Plant Cell. 1999; 11:1393–1404. [PubMed: 10449575]

17. Fu ZQ, et al. NPR3 and NPR4 are receptors for the immune signal salicylic acid in plants. Nature. 2012; 486:228–232. [PubMed: 22699612]

18. Cao H, Glazebrook J, Clarke JD, Volko S, Dong XN. The Arabidopsis NPR1 gene that controls systemic acquired resistance encodes a novel protein containing ankyrin repeats. Cell. 1997; 88:57–63. [PubMed: 9019406]

19. Tada Y, et al. Plant immunity requires conformational changes [corrected] of NPR1 via S-nitrosylation and thioredoxins. Science. 2008; 321:952–956. [PubMed: 18635760]

20. Jahan MS, et al. Deficient glutathione in guard cells facilitates abscisic acid-induced stomatal closure but does not affect light-induced stomatal opening. Bioscience, biotechnology, and biochemistry. 2008; 72:2795–2798.

21. Despres C, et al. The Arabidopsis NPR1 disease resistance protein is a novel cofactor that confers redox regulation of DNA binding activity to the basic domain/leucine zipper transcription factor TGA1. Plant Cell. 2003; 15:2181–2191. [PubMed: 12953119]

22. Mas P, Alabadi D, Yanovsky MJ, Oyama T, Kay SA. Dual role of TOC1 in the control of circadian and photomorphogenic responses in Arabidopsis. Plant Cell. 2003; 15:223–236. [PubMed: 12509533]

23. Millar AJ, Carre IA, Strayer CA, Chua NH, Kay SA. Circadian clock mutants in Arabidopsis identified by luciferase imaging. Science. 1995; 267:1161–1163. [PubMed: 7855595]

24. Zhang C, et al. Crosstalk between the Circadian Clock and Innate Immunity in Arabidopsis. PLoS Pathog. 2013; 9:e1003370. [PubMed: 23754942]

25. Wang W, et al. Timing of plant immune responses by a central circadian regulator. Nature. 2011; 470:110–114. [PubMed: 21293378]

26. Huang W, et al. Mapping the core of the Arabidopsis circadian clock defines the network structure of the oscillator. Science. 2012; 336:75–79. [PubMed: 22403178]

27. Wang D, Weaver ND, Kesarwani M, Dong X. Induction of protein secretory pathway is required for systemic acquired resistance. Science. 2005; 308:1036–1040. [PubMed: 15890886]

28. Shin J, Heidrich K, Sanchez-Villarreal A, Parker JE, Davis SJ. TIME FOR COFFEE represses accumulation of the MYC2 transcription factor to provide time-of-day regulation of jasmonate signaling in Arabidopsis. Plant Cell. 2012; 24:2470–2482. [PubMed: 22693280]

29. Baldwin IT, Meldau S. Just in time: circadian defense patterns and the optimal defense hypothesis. Plant signaling & behavior. 2013; 8:e24410. [PubMed: 23603968]

30. Nozue K, et al. Rhythmic growth explained by coincidence between internal and external cues. Nature. 2007; 448:358–361. [PubMed: 17589502]

31. Wang Y, et al. LIGHT-REGULATED WD1 and PSEUDO-RESPONSE REGULATOR9 form a positive feedback regulatory loop in the Arabidopsis circadian clock. Plant Cell. 2011; 23:486–498. [PubMed: 21357491]

32. Nakagawa T, et al. Development of series of gateway binary vectors, pGWBs, for realizing efficient construction of fusion genes for plant transformation. Journal of bioscience and bioengineering. 2007; 104:34–41. [PubMed: 17697981]

33. Clough SJ, Bent AF. Floral dip: a simplified method for Agrobacterium-mediated transformation of Arabidopsis thaliana. The Plant journal : for cell and molecular biology. 1998; 16:735–743. [PubMed: 10069079]

34. Queval G, Noctor G. A plate reader method for the measurement of NAD, NADP, glutathione, and ascorbate in tissue extracts: Application to redox profiling during Arabidopsis rosette development. Analytical biochemistry. 2007; 363:58–69. [PubMed: 17288982]

35. Deplancke B, Dupuy D, Vidal M, Walhout AJ. A gateway-compatible yeast one-hybrid system. Genome research. 2004; 14:2093–2101. [PubMed: 15489331]

36. Pruneda-Paz JL, Breton G, Para A, Kay SA. A functional genomics approach reveals CHE as a component of the Arabidopsis circadian clock. Science. 2009; 323:1481–1485. [PubMed: 19286557]

37. Gendrel AV, Lippman Z, Yordan C, Colot V, Martienssen RA. Dependence of heterochromatic histone H3 methylation patterns on the Arabidopsis gene DDM1. Science. 2002; 297:1871–1873. [PubMed: 12077425]

38. Schmittgen TD, Livak KJ. Analyzing real-time PCR data by the comparative C(T) method. Nature protocols. 2008; 3:1101–1108. [PubMed: 18546601]

39. Dodd AN, Dalchau N, Gardner MJ, Baek SJ, Webb AA. The circadian clock has transient plasticity of period and is required for timing of nocturnal processes in Arabidopsis. The New phytologist. 2014; 201:168–179. [PubMed: 24102325]

40. Finkenstadt B, et al. Reconstruction of transcriptional dynamics from gene reporter data using differential equations. Bioinformatics. 2008; 24:2901–2907. [PubMed: 18974172]

41. Edwards KD, et al. Quantitative analysis of regulatory flexibility under changing environmental conditions. Molecular systems biology. 2010; 6:424. [PubMed: 21045818]

42. Farre EM, Harmer SL, Harmon FG, Yanovsky MJ, Kay SA. Overlapping and distinct roles of PRR7 and PRR9 in the Arabidopsis circadian clock. Current biology : CB. 2005; 15:47–54. [PubMed: 15649364]

43. Rand DA, Shulgin BV, Salazar D, Millar AJ. Design principles underlying circadian clocks. Journal of the Royal Society, Interface/the Royal Society. 2004; 1:119–130.
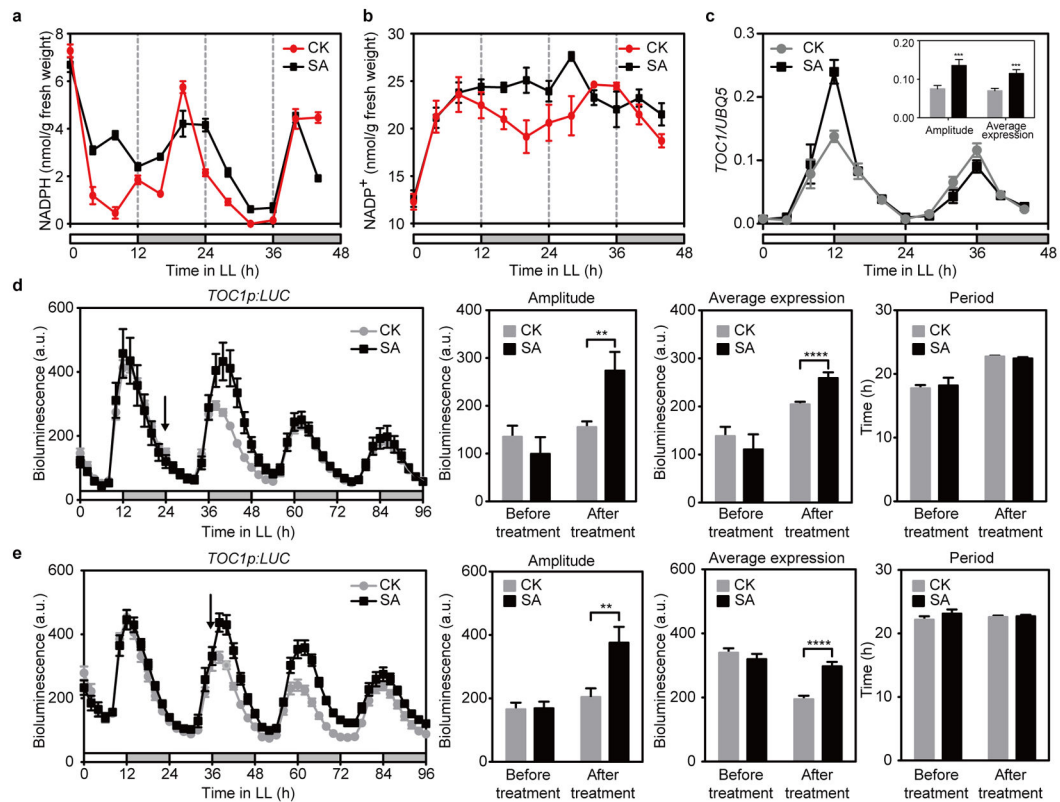
Figure 1. SA disrupts redox rhythm but boosts *TOC1* expression without changing its period
a–c, NADPH (**a**), NADP$^+$ (**b**) and *TOC1* mRNA (**c**) in plants after application of water (CK) or SA at 0 h under constant light (LL). White and grey bars represent subjective days and nights, respectively. Data are mean ± s.e.m. (*n* = 3; *t*-test; ***, *P* < 0.001). **d, e,** *TOC1p:LUC* activity rhythms in plants treated with water (CK) or SA at subjective dawn (**d**) and dusk (**e**) (mean ± s.e.m.; *n* = 6). Arrows indicate treatment time. a.u., arbitrary unit. Bar graphs represent mean ± s.e.m. (Holm-Sidak test; **, *P* < 0.01; ****, *P* < 0.0001).
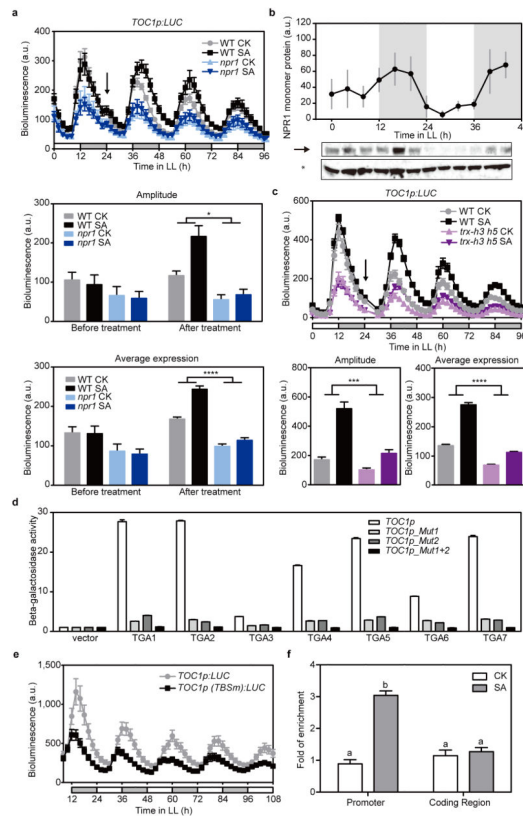
Figure 2. SA-regulation of *TOC1* depends on nuclear NPR1

a, c, *TOC1p:LUC* activity rhythms in wild-type (WT) and *npr1-3* (**a**) or *trx-h3 trx-h5* (*trx-h3 h5,* **c**) treated with water (CK) or 1 mM SA at subjective dawn (arrow) under constant light (mean ± s.e.m.; *n* = 6). Bar graphs show mean ± s.e.m. (two-way ANOVA; *, *P* < 0.05; ***, *P* < 0.001; ****, *P* < 0.0001). **b,** NPR1 monomer (arrow) quantified using the non-specific bands (*) as a loading control. Data are mean ± s.e.m. (*n* = 3). **d,** Beta-galactosidase reporter activities shown as fold changes over the vector control. Mut1 and Mut2, mutants of two TGA-binding sites (TBSm). Data are mean ± s.e.m. (*n* = 3). **e,** Luciferase activity rhythms of *TOC1p:LUC* and *TOC1p(TBSm):LUC* (mean ± s.e.m., *n* = 20 T1-transformants). **f,** ChIP experiments were performed using *35S:NPR1-GFP* (in *npr1-1*) plants. Data are mean ± s.e.m. (*n* = 3; Tukey's multiple comparisons test; *P* < 0.0001).
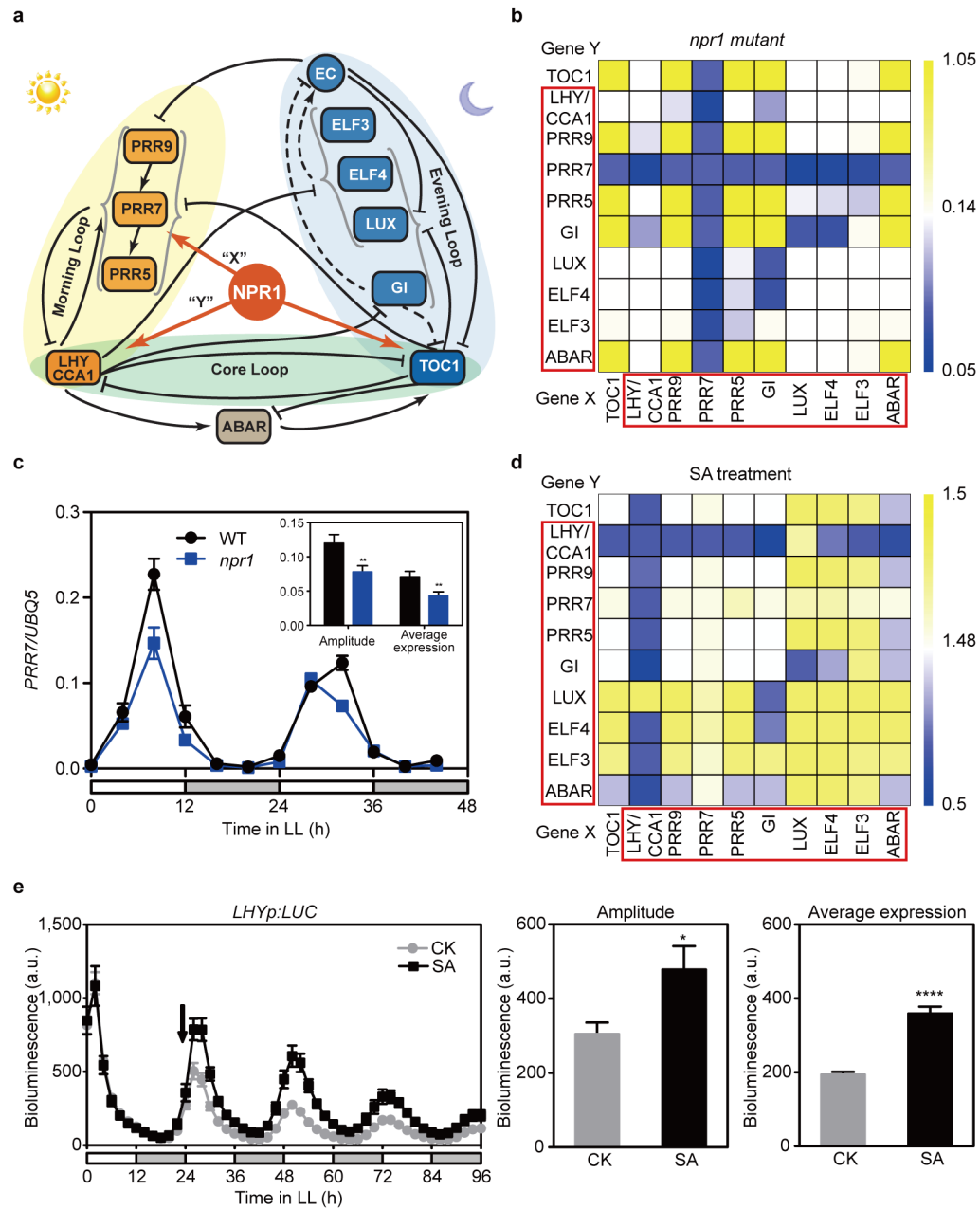
**Figure 3. NPR1 regulates transcription of multiple clock genes**

a, NPR1 regulates transcription of genes in the P2012 version of *Arabidopsis* TTFL clock[13]. "X", "Y", query genes for mathematical modelling. Arrows, transcriptional activation. Block arrows, repression. Dashed lines, post-translational interactions or regulation. **b, d,** The least squares fitting results of different query genes (X,Y) to the *npr1* data (**b**) and the SA-treated wild-type data (**d**) in Fig. 2a. The colour bars indicate the least squares residual for each gene combination. Lower residual indicates a better fit. **c**, *PRR7* mRNA in WT and *npr1*. Data are mean ± s.e.m. (*n* = 3; *t*-test; **, *P* < 0.01). **e,** *LHYp:LUC* activity rhythms in plants treated with water (CK) or SA at subjective dawn (arrow) (mean ± s.e.m.; *n* = 6). Bar graphs represent mean ± s.e.m. (*t*-test; *, *P* < 0.05; ****, *P* < 0.0001).
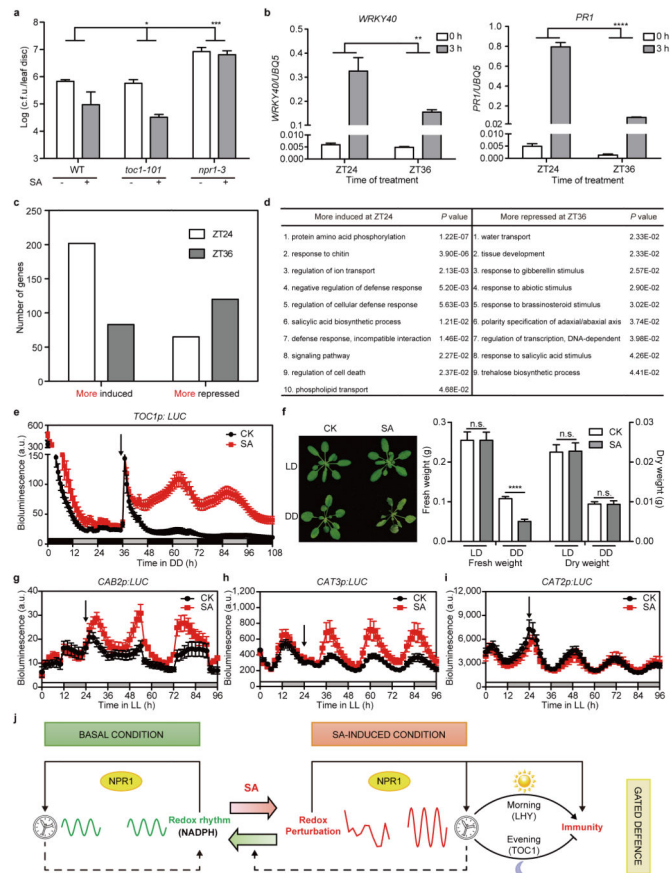
Figure 4. SA reinforces the circadian clock to gate immune response

a, *Pseudomonas syringae* pv. *maculicola* ES4326 growth in plants pre-treated with water (−) or SA (+) (24 hours) 3 days post infection. c.f.u., colony-forming units. Data are mean ± 95% confidence intervals (*n* = 8; two-way ANOVA; *, *P* < 0.05; ***, *P* < 0.001). **b,** *WRKY40* and *PR1* expression in plants 0 or 3 hours (h) after SA treatment. Data are mean ± s.e.m. (*n* = 3; two-way ANOVA; **, *P* < 0.01; ****, *P* < 0.0001). **c,** Time-of-day-specific transcriptome changes in response to SA treatment. **d,** Enriched gene ontology categories. **e,** **g,** *TOC1p:LUC* (**e**), *CAB2p:LUC*, *CAT3p:LUC* and *CAT2p:LUC* (**g**) activity rhythms in water (CK)- or SA-treated plants (mean ± s.e.m.; *n* = 11 in **e** and n = 6 in **g**). DD, constant dark. Darker and lighter bars represent subjective days and nights, respectively. **f,** Symptom (left) and fresh/dry weight (right) of plants treated with water (CK) or SA under constant dark (DD) or diurnal conditions (LD) (mean ± s.e.m.; *n* = 6; *t*-test; ****, *P* < 0.0001; n.s., non-significant). **h,** A model showing the interactions between redox and the circadian clock in gating defence.